Ab initio calculations for point defect clusters with P, As, and Sb in Si

Beat Sahli, Kilian Vollenweider, and Wolfgang Fichtner
Integrated Systems Laboratory, ETH Zurich, Gloriastrasse 35, 8092 Zurich, Switzerland
(Received 20 April 2009; revised manuscript received 24 June 2009; published 25 August 2009)

We present results of *ab initio* calculations for point defect clusters with phosphorus, arsenic, and antimony in silicon, including mixed clusters. We show that these dopant species interact, modifying their diffusion and activation. Most importantly, mixed clusters can exist in similar concentrations as pure clusters, reducing the fraction of active dopants. Furthermore, we analyze the influence of cluster composition on the configurations and energetics. Phosphorus and arsenic atoms take similar roles in the cluster configurations, whereas antimony leads to different configurations. The binding to self-interstitials is weaker for As than for P and weaker for Sb than for As. The binding to a vacancy is stronger for As than for P and stronger for Sb than for As. For all clusters with one vacancy and up to four dopant atoms, the constant binding energy per dopant atom is −1.17 eV for P, −1.27 eV for As, and −1.34 eV for Sb. Finally, we derive reaction enthalpies from the calculated formation energies and discuss the implications for dopant diffusion and activation.

DOI: 10.1103/PhysRevB.80.075208 PACS number(s): 68.55.Ln, 31.15.es, 61.72.J−

I. INTRODUCTION

The ongoing scaling of integrated circuits to ever-smaller feature size requires a detailed understanding of the physical processes during manufacturing. Phosphorus, arsenic, and antimony are the three important *n*-type dopants for silicon technologies. They differ in characteristics relevant for semiconductor technology, e.g., the diffusion coefficient, the solid solubility, or their behavior in ion implantation. Selecting the optimal dopant for a specific application is a complex problem, depending on the changing requirements for state-of-the-art manufacturing technologies. For example, antimony has recently gained special attention because of its advantageous behavior in strained silicon.[1,2] The ever increasing requirements for semiconductor technology even call for solutions with several *n*-type dopant species in the same region of the device, cleverly combining the respective advantages and disadvantages of the individual dopant species.[3–5] The diffusion and activation behavior of one dopant species may also be modified by the presence of another dopant species. Therefore, the interaction between the different dopant species must be investigated. This interaction can be indirect, via clusters with self-interstitials (I) or vacancies (V), or direct, via mixed clusters (containing several dopant species). Comprehensive diffusion and clustering models must properly include mixed clusters.

Process simulation is a vital tool for the development and optimization of advanced microelectronic devices. For the manufacturing of advanced devices, an essential step is the formation of highly doped ultrashallow junctions, where a complex system of diffusing and reacting defects in the silicon wafer is involved. The accurate simulation of the resulting dopant diffusion and dopant cluster formation is an important part of process optimization. The diffusion and clustering models in state-of-the-art process simulators, based on either the kinetic Monte Carlo (KMC) or the continuum approach, require the relevant physical properties of the involved defects as input parameters.[6] The experimental determination of all required atomic-level properties for the large number of important defects is currently not possible. Therefore, *ab initio* calculations of such defect properties such as formation energies or binding energies are of great interest for the development of dopant diffusion and clustering models.

The goal of this study is to investigate the clustering of As, P, and Sb in Si with *ab initio* calculations based on density-functional theory (DFT), including mixed clusters with two types of dopant atoms. Numerous previous *ab initio* calculations have been performed for these three dopants. Many studies considered only defects with dopant-vacancy or dopant-interstitial pairs or other small clusters.[7–16] Several studies also included larger clusters with only As dopant atoms[17–26] and one study included AsPV, a defect with two different dopant species.[27] However, there have been no previous *ab initio* studies for larger P clusters, Sb clusters, or mixed clusters. In summary, the clustering of Sb and the mixed clustering of P, As, and Sb has not yet been investigated in a consistent manner with *ab initio* methods.

The overall goal of our project is to gain a broad understanding of defect diffusion and clustering in silicon. An important part is to create a comprehensive database of *ab initio* results, concentrating on the relevant defect properties. The selection of defects and the details of the computational setup are geared toward maximizing the gain of knowledge useful for the understanding of dopant clustering and diffusion. Our approach was to investigate a large number of potentially important defects to allow for the discovery or confirmation of trends or general rules in the clustering energetics and defect configurations. This was achieved by consistently using the same computational setup for all defects. Since hundreds of calculations have been performed, some of the work had to be automated.

In process simulation, the goal is to determine the system state after annealing with a limited thermal budget. During annealing, the system of dopants and defects in the silicon crystal is not in complete equilibrium. For example, immediately after ion implantation, a region with a large supersaturation of self-interstitials exists. These interstitials form clusters with dopant atoms that are rare under equilibrium conditions. Since there are still (steep) gradients in the dopant concentration in the finished device, the system is not in

 ©2009 The American Physical Society

complete equilibrium even after the annealing. Process simulation must determine the evolution of a complex reaction-diffusion system with many defects species and possible reactions, starting from initial conditions influenced by the ion implantation parameters. Therefore, KMC simulations with all considered defects will be required for a complete analysis of the implications of the clustering energetics presented in this paper. Nevertheless, we can directly make important conclusions by calculating binding energies and reaction enthalpies. The resulting qualitative statements represent significant physical insights and are a valuable basis for detailed investigations with KMC models based on the calculated clustering energetics.

II. METHODS

For each defect species that can be formed by a reaction, the configuration with the lowest energy must be determined. The search is performed as usual by starting relaxations (local energy minimization) from several different initial configurations. Simply searching for the lowest energy supercell containing the right number of dopants would yield wrong configurations for defects with repulsive constituents (an example is discussed in Sec. III D). The cluster constituents would be separated. We must exclude configurations not attainable by reactions. Since the computational cost of molecular-dynamics simulations of reactions is prohibitive, we have to apply a criterion based on the cluster geometry. The selection of this criterion is arbitrary and it is not guaranteed that the correct configurations are considered. We used a criterion based on the Voronoi cells of the perfect silicon lattice.[28] Each Voronoi cell that does not contain exactly one silicon atom was marked as defective. Two Voronoi cells were defined to be connected when they belong to first- or second-nearest-neighbor lattice sites. A set of connected defective Voronoi cells was considered to represent one defect.

In accordance with the conventional approach in *ab initio* studies of point defects and dopant clustering, the formation energy $E_f[X]$ of defect X was calculated with

$$E_f[X] = E_{tot}[X] - \sum_i n_i \mu_i, \tag{1}$$

where $E_{tot}[X]$ is the total energy of the supercell containing the defect, n_i is the number of atoms of type i in the supercell, and μ_i is the corresponding chemical potential.[29] In the dilute case, the equilibrium concentration of defect X is then

$$C_{eq}[X] = C_0[X] e^{-E_f[X]/kT}. \tag{2}$$

In the present study, no actual defect concentrations are calculated because the prefactors $C_0[X]$ depend on the formation entropies (and on the concentrations of possible sites), which were not investigated. Furthermore, the formation energies depend on the chemical potentials μ_i, which in turn depend on the environmental constraints of the system, i.e., if atoms of type i can be exchanged with a reservoir or if their total concentration is fixed.

As discussed in Sec. I, we investigate dopant clustering during semiconductor device manufacturing, in particular, during annealing after ion implantation. The system is not in complete equilibrium and the total concentrations and chemical potentials of the dopant species vary throughout the device. A rough approximation is to assume that the clustering reactions are in equilibrium in a spatially limited area of the device with a fixed total concentration for each dopant species. These total concentrations determine the chemical potentials at this point. Such an approximation must be considered with great care. To achieve equilibrium between cluster types, there must be mobile defects to transport their constituents. These mobile defects also change the local total concentration. Whether there is a sufficiently large separation between the two respective time scales depends on many factors, including defect mobilities and concentration gradients. Such a calculation is correct only when all dominant clusters are included in the calculation. Otherwise, the results for the included clusters are overestimated. For these reasons, it is better to analyze the clustering energetics in ways that are independent of the chemical potentials.

Total binding energies and reaction enthalpies are derived from the formation energies. They are independent of the chemical potentials since the numbers of atoms are conserved in the reactions. Therefore, pathways for cluster formation and the binding strength between cluster constituents can be investigated without specifying values for the chemical potentials. Since there are many possible reactions for each defect, we will not list all reaction enthalpies. Instead, we present the formation energies for a specific choice of the chemical potentials. We used $\mu_{Si} = \frac{E_{tot}[Si]}{N}$ for silicon atoms and $\mu_D = E_{tot}[D] - (N-1)\mu_{Si}$ for dopant atoms, where $E_{tot}[Si]$ is the total energy of a supercell with no defect, N is the number of lattice sites in the supercell, and $E_{tot}[D]$ is the total energy of the supercell with one substitutional dopant atom. With these definitions, the formation energy includes the energy required to assemble the cluster from its isolated constituents and the energy required to create the isolated vacancies or interstitials. The selected definitions allow the comparison of our results to the most comprehensive previous study of As clusters.[22]

The calculations were performed with the DFT-based Vienna *ab initio* simulation package (VASP).[30,31] Cubic supercells with 216 lattice sites were used. The lattice constant was set to the calculated value of 5.47 Å. All defects were considered in the neutral charge state. The generalized gradient approximation was used (Perdew-Wang 91) together with the projector-augmented wave method.[32] The cutoff energy for the plane-wave expansion was set to 191.312 eV. The Brillouin zone was sampled only at the Γ point. The conjugate gradient algorithm was used to relax the atomic positions, stopping when the energy difference between two steps was less than 10^{-3} eV.

In order to estimate the numerical accuracy of the results for the formation energies, we performed calculations for a subset of the clusters with a plane-wave cutoff energy of 270 eV and a $3\times3\times3$ Monkhorst-Pack k-point grid.[33] A comparison of the two sets of results in Fig. 1 indicates that our calculations do indeed represent the predictions within the framework of DFT. We conclude that the observed trends can be considered as independent of the details of the computational setup, as long as a reasonable setup is consistently

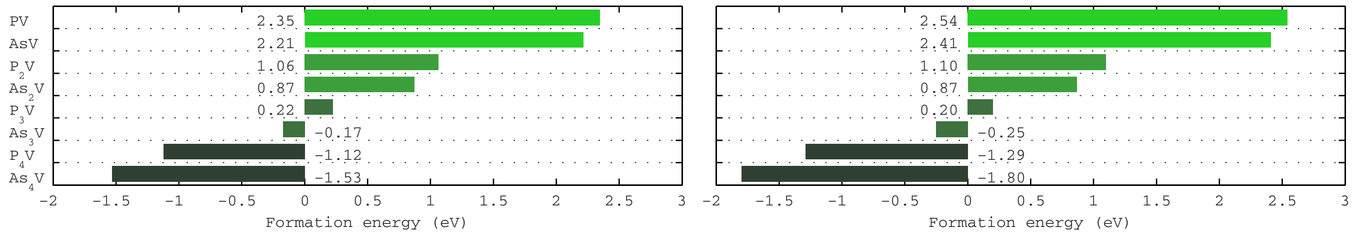

FIG. 1. (Color online) Comparison of formation energies of selected clusters (with simple configurations) calculated with different k-point sampling and plane-wave energy cutoff. Left: Γ point and 191.312 eV. Right: $3\times3\times3$ Monkhorst-Pack and 270 eV.

used for all calculations. Furthermore, for each defect, either the absolute difference is below 0.1 eV or the relative difference is below 15%. Considering this error estimation, our results for the As clusters are in good agreement with the formation energies reported in Ref. 22.

III. RESULTS AND DISCUSSION

In the following, D_n is used to denote a group of in total n dopant atoms with arbitrary numbers of P, As, or Sb atoms.

A. Defect configurations

The large number of defects considered prohibits a detailed discussion of all minimum-energy configurations. We describe the basic structure of all defects and for several selected defects we include a more detailed description of the lattice relaxations and discuss basic trends that hold for the other defects as well. Several defect configurations are shown graphically. In these plots, Si, P, As, and Sb atoms are represented by blue (small, light), red (small, dark), green (medium size), and pink (large) spheres, respectively. The plots also include the bonds of a reference lattice shown as gray cylinders. The bonds are not drawn between actual atom positions but between the positions of the undisturbed lattice sites. This increases the visibility of the lattice relaxations. For example, in Fig. 2(a) it is clearly visible that the distance between the two neighboring P atoms is larger than the bond length of the undisturbed Si lattice.

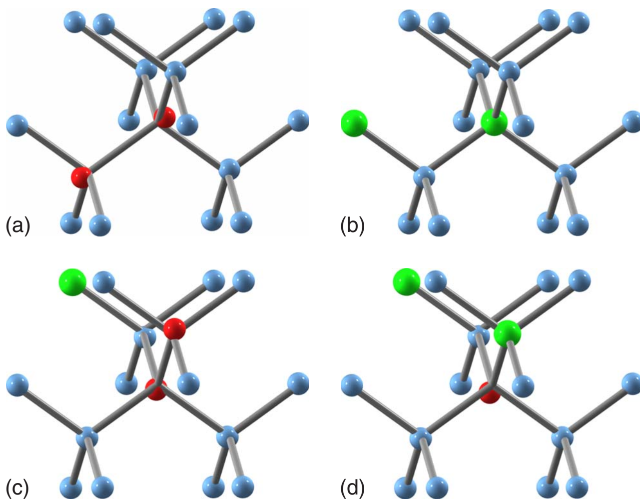

FIG. 2. (Color online) Configurations of selected clusters of substitutional dopants.

1. Clusters of substitutional dopants

In defects without I or V, all dopant atoms are on lattice sites (substitutional). Several examples are shown in Fig. 2. The clusters of type D_2 and D_3 have a higher total energy compared to isolated substitutional dopants. Due to our Voronoi cell based criterion, we considered only configurations with the dopant atoms on first- or second-nearest-neighbor lattice sites of each other. For P_2 and PAs, the two dopants are on first-nearest-neighbor lattice sites since the energy of the second-nearest-neighbor configuration is higher. For all other defects of type D_2, the second-nearest-neighbor position has the lower energy.

For all D_3 clusters, two dopant atoms are first nearest neighbors and the third one is on a second-nearest-neighbor position of the central one, as shown in Fig. 2(c). When different dopant species are present, the dopant atom on the second-nearest-neighbor position is always one with the larger atomic radius and the central dopant atom is always one with the smaller atomic radius.

Although all atoms are on lattice sites, the lattice relaxes around the impurities. Figure 3 depicts the lattice relaxations around the three isolated substitutional dopants. The lattice relaxation increases with the increasing atomic radii of P, As, and Sb. The first nearest neighbors of the As and Sb dopant atoms show clear outward relaxation. Compared to the undisturbed bond length of 2.37 Å, the relaxation around P is very small and the relaxation around Sb is significant. In all three cases, the relaxations rapidly decrease with increasing distance from the dopant atom. They reach very small values for interatomic distances clearly below the maximum possible in supercells with 216 lattice sites. The relaxations are predominantly in the radial direction. The second nearest neighbors of the dopant atoms exhibit the strongest perpendicular relaxation.

2. Clusters with dopants and one vacancy

For all clusters of type $D_xV(x=1,2,3,4)$, the dopant atoms are positioned on the first-nearest-neighbor positions of the vacant lattice site. Two representative examples, P_3V and $SbAs_2V$, are shown in Fig. 4. The inward relaxation of the dopants toward the vacancy is apparent. The relaxation increases with the increasing atomic radii of P, As, and Sb. Figure 5 depicts the relaxations for three other examples (P_3SbV, P_2Sb_2V, and As_4V) in more detail, confirming the

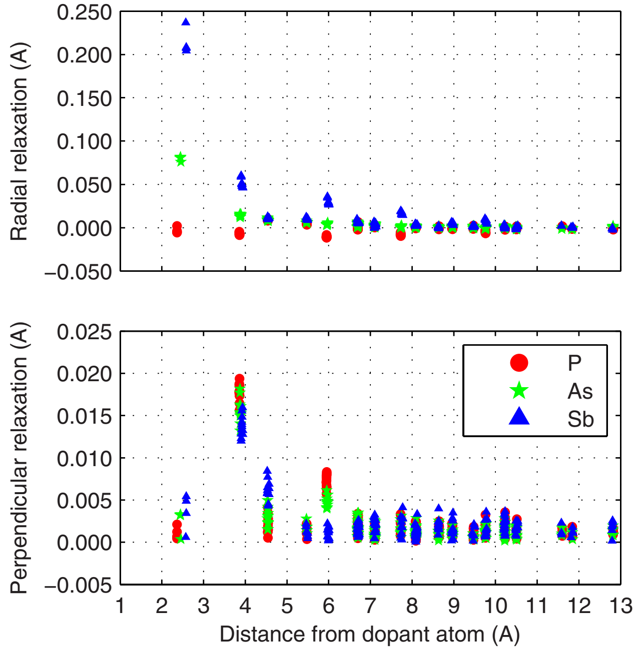

FIG. 3. (Color online) Lattice relaxations around a single substitutional P, As, or Sb atom. The distance of all other atoms in the simulation cell to the dopant atom is shown on the x axis. In the upper plot, the y axis shows the radial displacement of the atom from the closest lattice site. Negative and positive values represent inward and outward relaxations, respectively. In the lower plot, the y axis shows the displacement perpendicular to the radial displacement.

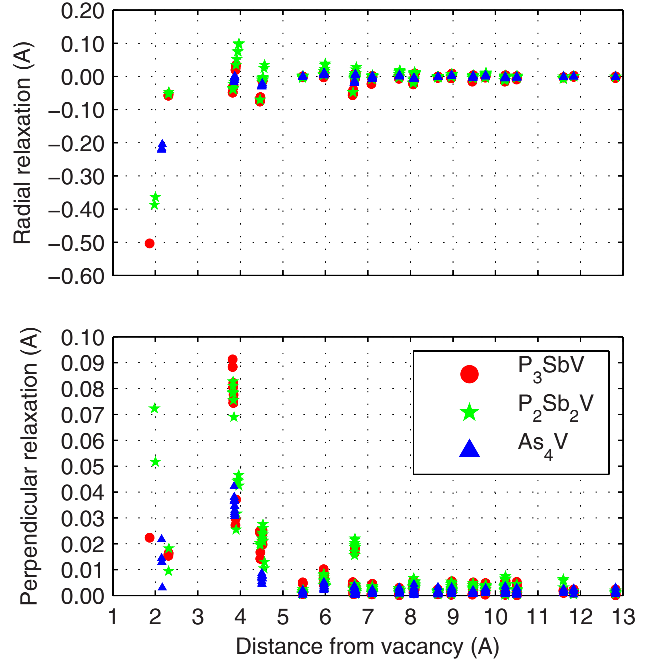

FIG. 5. (Color online) Lattice relaxations around a vacancy. Analogous to Fig. 3 but the x axis shows the distance of all atoms in the simulation cell to the vacant lattice site.

trend. The relaxation is stronger than around the isolated substitutional dopants. Again, the relaxations are predominantly in the radial direction and they fall off rapidly with increasing distance to the vacancy.

3. Clusters with dopants and one interstitial

DI clusters have a split ⟨110⟩ configuration. While P and As are part of the split pair as shown in Fig. 6(a), Sb has a substitutional position next to the split pair as shown in Fig. 6(b).

D_2I clusters without Sb have split configurations as well, slightly tilted from the ⟨110⟩ direction, with both dopant atoms part of the split pair, as shown in Fig. 6(c). In D_2I clusters with one Sb atom, the Sb atom is sitting on a lattice site and the As or P atom is part of a distorted split ⟨110⟩ structure centered on a second-nearest-neighbor lattice site, as shown in Fig. 6(d). The configuration of Sb_2I is an extended split ⟨110⟩ as shown in Fig. 6(e).

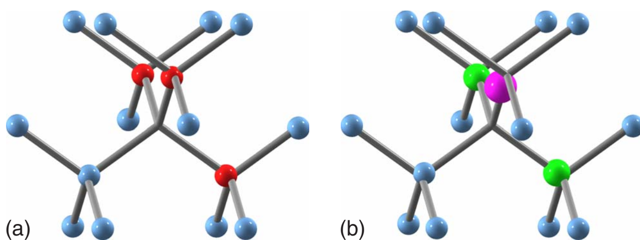

FIG. 4. (Color online) Configurations of selected clusters with dopants and one vacancy.

In the cluster Sb_3I, one Sb atom is part of a split ⟨110⟩ pair and the other two Sb atoms are on two second-nearest-neighbor positions of the split lattice site, as shown in Fig. 6(f). For P_3I and As_3I, two dopant atoms are part of a tilted split ⟨110⟩ and the third dopant atom is on a first-nearest-neighbor lattice site, as shown in Fig. 6(g). For all other clusters of type D_3I, two dopant atoms are part of a tilted split ⟨110⟩ and the third dopant atom is on one of the second-nearest-neighbor lattice sites (not always the same). An example is shown in Fig. 6(h).

4. Clusters with dopants and two interstitials

In DI_2 clusters, the dopant atom shares one lattice site together with two Si atoms. The configuration for PI_2 is shown in Fig. 7(a). AsI_2 has a very similar structure. The configuration of SbI_2 is shown in Fig. 7(b).

B. Formation energies

The calculated cluster formation energies are summarized in Fig. 8. Because of our particular choice for the chemical potentials of the dopant species, the formation energies of substitutional P, As, and Sb are zero and not included in the plot. Defects with the same number of dopant atoms and vacancies or interstitials are shown in the same color.

For clusters including a vacancy, the formation energy decreases when a P atom is replaced by an As or Sb atom, or when an As atom is replaced by an Sb atom. For clusters including an interstitial, the formation energy increases when a P atom is replaced by an As or Sb atom, or when an As atom is replaced by an Sb atom.

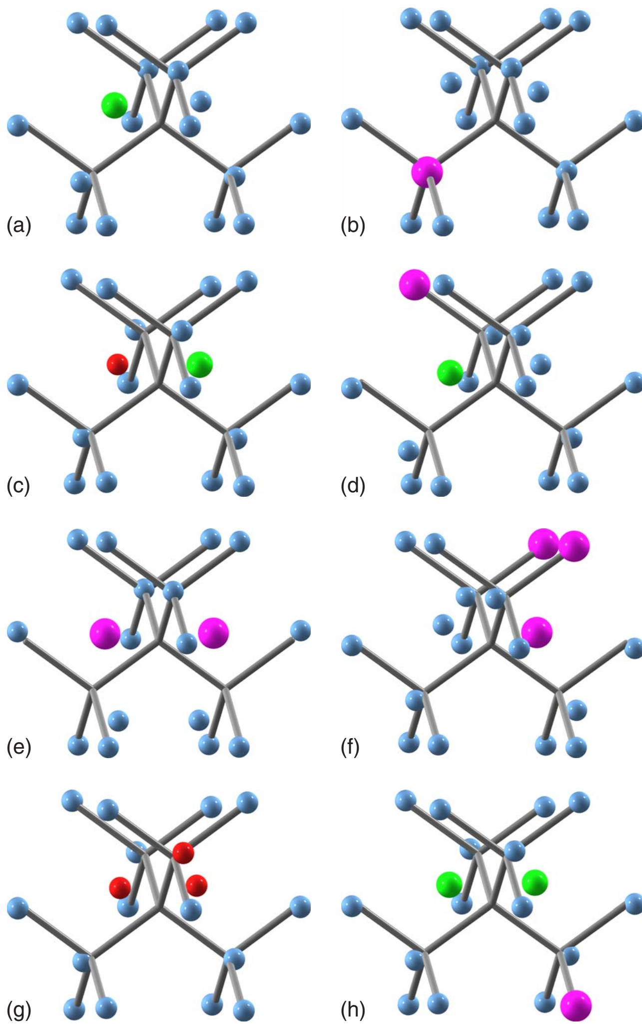

FIG. 6. (Color online) Configurations of selected clusters with dopants and one interstitial.

Similar to the lattice relaxations, the trends in the formation energies are consistent with the different atomic sizes of the three dopants. A vacancy represents available space in the lattice. Moving it next to a large dopant atom reduces the system energy more than moving it next to a smaller dopant atom. An interstitial represents missing space in the lattice. Combining it with smaller dopant atoms is energetically favorable.

There is a direct interaction between different dopant species. The existence of mixed clusters significantly increases the total number of available defect species. For example,

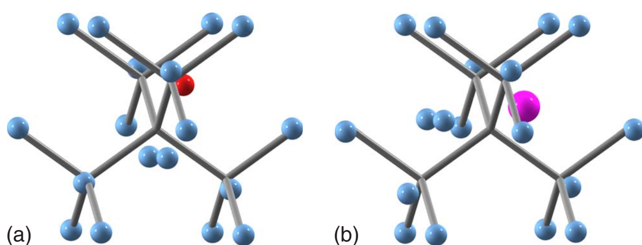

FIG. 7. (Color online) Configurations of selected clusters with dopants and two interstitials.

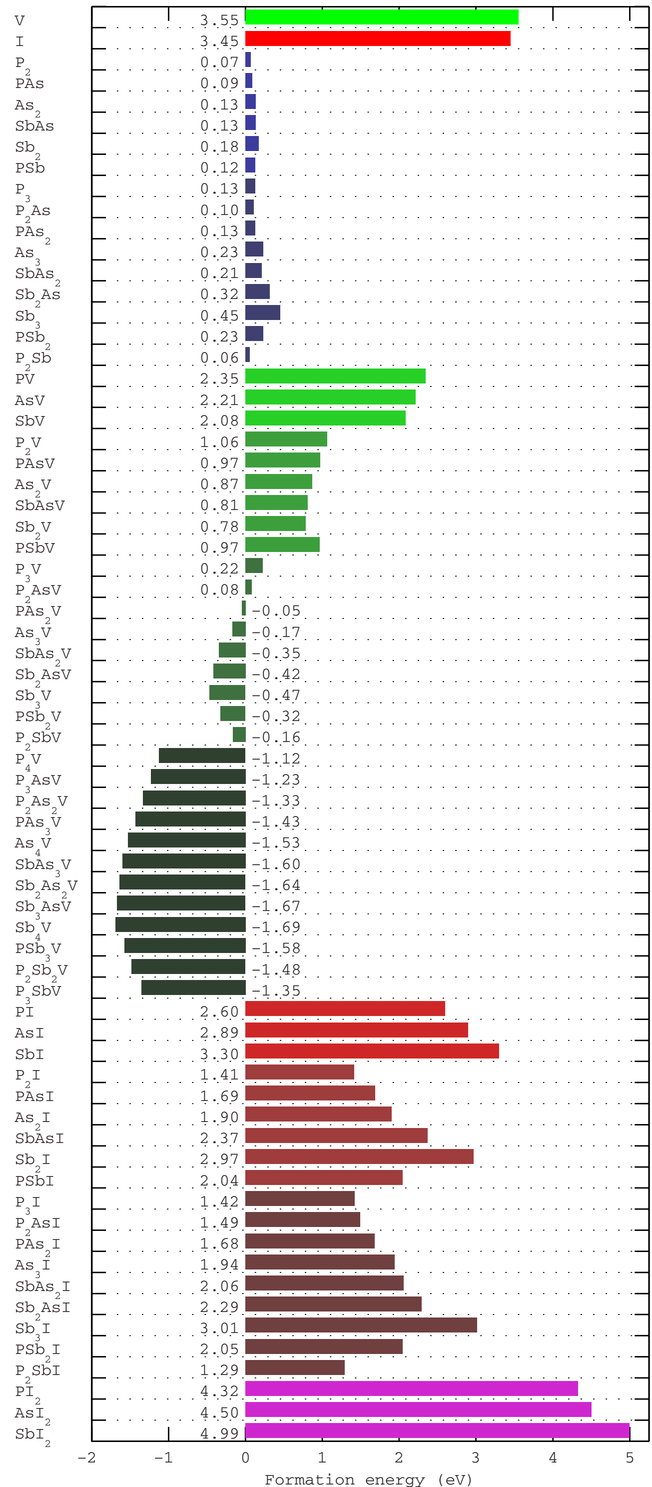

FIG. 8. (Color online) Formation energy; the numerical values are written next to the corresponding bars.

there are only three pure but nine mixed clusters of type D_4V. When a fixed concentration of dopant atoms is distributed to a larger number of defect species, the fraction in the individual defect species is reduced, including the fraction of substitutional dopants. This effect is only significant if the concentrations of the added mixed clusters are not negligible. Mixed clusters have similar formation energies as pure clusters. Switching one dopant of a pure cluster with a substitu-

tional dopant of another kind does not involve a large change in energy. Therefore, if the different dopant species are present in similar concentrations, mixed clusters exist in similar concentrations as pure clusters.

The formation energy of all D_4V and some D_3V clusters is negative. With our particular choice for the chemical potentials, we interpret these negative formation energies as follows: the energy gained from binding the dopants to a vacancy is larger than the energy required to form a vacancy. For fixed dopant concentrations, this provides a mechanism to lower the fraction of active dopants, especially for lower annealing temperatures.

The formation energies of the investigated defects cover a range of more than 6 eV. For example, typical changes in energy when replacing one dopant with another in D_4V type clusters are on the order of 0.1 eV. Energy differences between clusters of different types are typically much larger. Considering that energy differences usually appear in the form of $e^{\Delta E/kT}$ and $kT=0.112$ eV at a high annealing temperature of 1300 K, it is clear that the observed trends in the clustering energetics lead to significant effects in the clustering behavior.

C. Binding energies

The total binding energy is defined as the energy consumed when forming the defect from isolated substitutional dopants and vacancies or self-interstitials. This is identical to the definition of the total binding energy (or potential energy) used in KMC simulations for semiconductor processing applications.[6,34] An overview of our results is shown in Fig. 9.

(1) The binding to vacancies is stronger for As than for P and stronger for Sb than for As. The binding to self-interstitials is weaker for As than for P and weaker for Sb than for As.

(2) It is energetically favorable to add a P, As, or Sb dopant to any of the DV, D_2V, or D_3V clusters. However, substitutional dopants and D_2V and D_3V clusters are generally considered to be immobile, restricting such direct cluster-growth reactions (see below).

The binding energy per atom is an interesting characterization of clusters with only one type of constituent. To extract the binding energy per dopant atom (ϵ_P, ϵ_{As}, and ϵ_{Sb}) in clusters of type $D_xV(x=n_P+n_{As}+n_{Sb}=1,2,3,4)$ we used the simple linear model

$$E_b = n_P\epsilon_P + n_{As}\epsilon_{As} + n_{Sb}\epsilon_{Sb}, \quad (3)$$

where n_P, n_{As}, and n_{Sb} are the numbers of P, As, and Sb atoms in the cluster, respectively. A least-squares fit to the calculated binding energies yields $\epsilon_P=-1.17$ eV, $\epsilon_{As}=-1.27$ eV, and $\epsilon_{Sb}=-1.34$ eV. In Fig. 10, the binding energies according to the linear model are compared to the original formation energies. (It is a good but not perfect fit; the residuals are not independent.) This result confirms our observation that the binding to vacancies decreases with decreasing atomic weight: it is stronger for Sb than for As and stronger for As than for P. It would be interesting to perform equivalent calculations for larger clusters, i.e., D_xV_2 with $x=1,\ldots,6$. For our binding energies of clusters with dopants and interstitials, no good fit was obtained with a simple linear model.

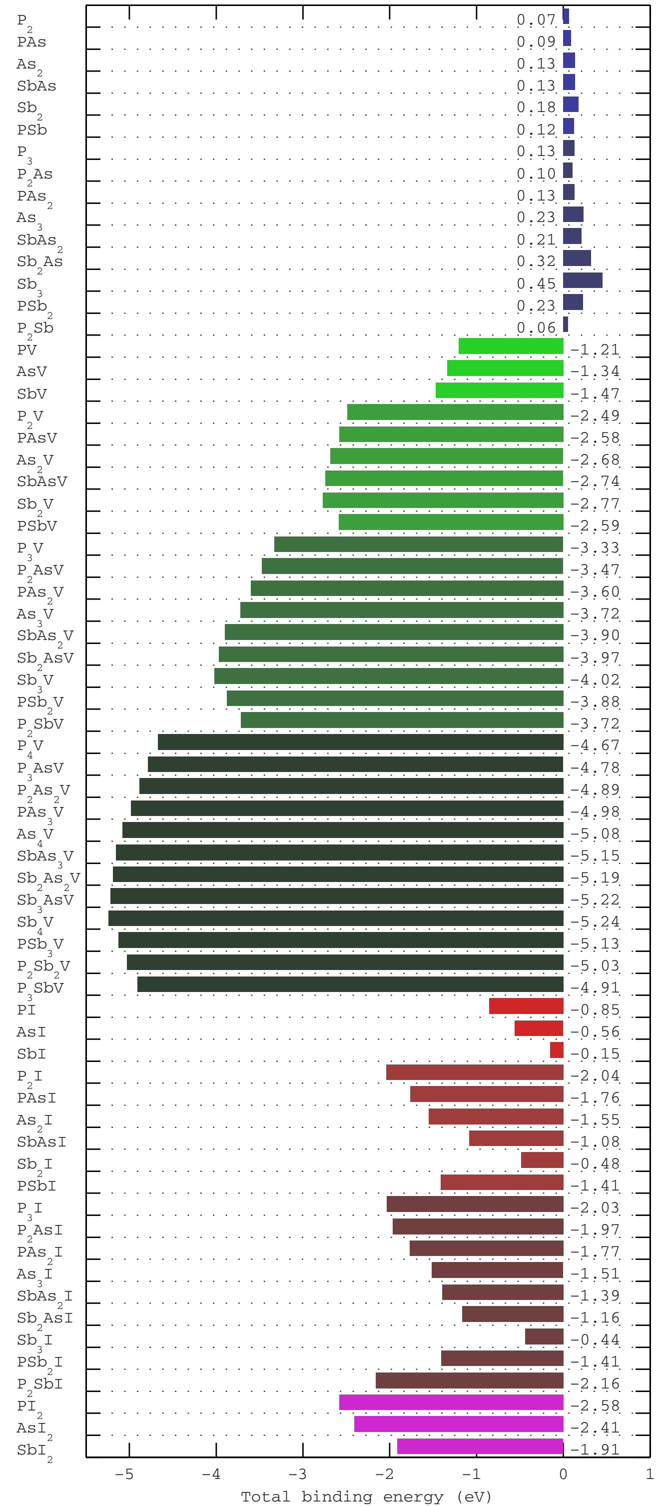

FIG. 9. (Color online) Total binding energy; the numerical values are written next to the corresponding bars.

D. Reaction enthalpies

The reaction enthalpy is the difference between the sum of the formation energies of the products and the sum of the

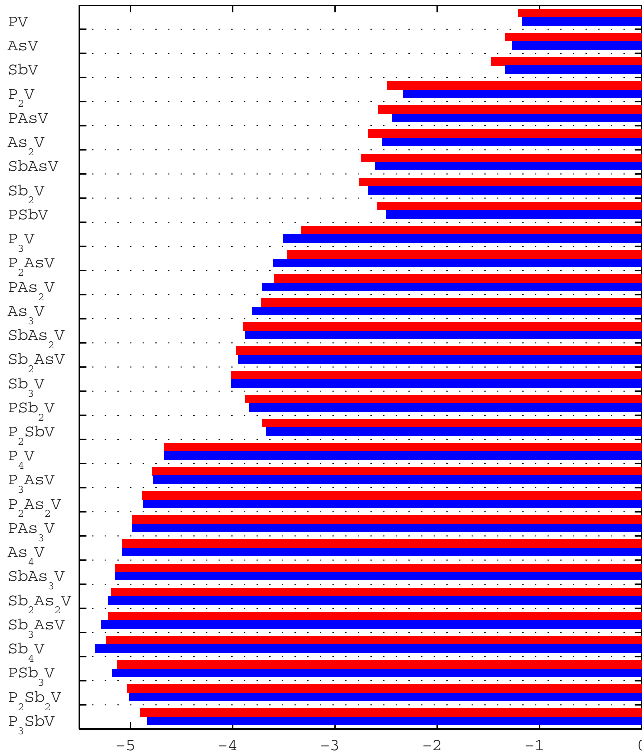

FIG. 10. (Color online) Comparison of the linear model of the total binding energy (lower bars, blue) and the original values (upper bars, red).

formation energies of the reactants. For example, in the reaction

$$P_2 + AsV \rightarrow P_2AsV \quad (4)$$

the amount of energy consumed in the forward reaction and released in the reverse direction is $E_f[P_2AsV]-(E_f[P_2]+E_f[AsV])=0.08\ \text{eV}-(0.07\ \text{eV}+2.21\ \text{eV})=-2.2\ \text{eV}$, i.e., the reaction is exothermic. On the other hand, the reaction

$$As_2I + As \rightarrow As_3I \quad (5)$$

is endothermic because it consumes 0.4 eV in the forward direction.

Repulsive clusters can be formed by exothermic reactions. For example, the reaction

$$PAsV + PI \rightarrow P_2As \quad (6)$$

involves a I-V pair recombination and releases 3.47 eV. The resulting dopant cluster has a higher total energy than isolated substitutional dopants. The dopant atoms repel each other. Reactions with other defects or spontaneous I-V pair generation are required to dissolve such clusters. They are relatively long lived and play important roles in the full clustering dynamics.

For two defects to react, at least one of them must be mobile so that they can approach each other. The set of possible reactions is therefore limited by the set of available mobile defects. Often, only the intrinsic point defects I and V and the pairs DI and DV are included in the set of potentially mobile defects. For this case, the enthalpies of 196 distinct reactions (with only one defect on the product side) are determined by the formation energies listed in Fig. 8. Additional defects may be mobile, as, for example, suggested by atomistic calculations for I_2 and I_3 (Refs. 35–38) or for As_2I.[21] The actual importance of such larger mobile defects depends on the specific application.[39] If all defects of type D_2I are also considered to be mobile, 211 distinct reactions are determined by the calculated formation energies. Among these, six reactions are slightly endothermic, including the reaction defined in Eq. (5).

Most of the clustering reactions are exothermic and therefore in a first approximation diffusion limited. There are many paths to form a specific cluster species with reaction rates depending on the concentrations and diffusivities of the building blocks. On the other hand, the rates of cluster dissolution reactions depend on the binding energies of the emitted defects. Therefore, mixed clusters can dissolve into mobile defects different to the ones from which they were built, effectively transforming the population of mobile defects. Dopant-vacancy clusters preferentially emit dopant-vacancy pairs with the largest dopant in the clusters. Dopant-interstitial clusters preferentially emit dopant-interstitial pairs with the smallest dopant.

IV. SUMMARY

We performed systematic *ab initio* calculations for a wide range of clusters with P, As, and Sb in Si. Using a consistent computational setup for all defects, we observed that P and As atoms take similar roles in the cluster configurations, whereas Sb leads to different atomic arrangements. The defect configurations and energetics depend, in a fundamental way, on the atomic sizes of the contained dopants. There is a direct interaction between the different dopant species. Mixed clusters can exist in similar concentrations as pure clusters. The concentration of active dopants can be reduced due to the increased number of possible cluster species. Binding to self-interstitials is weaker for As than for P and weaker for Sb than for As. The binding to vacancies is stronger for As than for P and stronger for Sb than for As. For D_4V clusters, the binding energy per dopant atom is −1.17 eV for P, −1.27 eV for As, and −1.34 eV for Sb. Dopant-vacancy clusters preferentially emit dopant-vacancy pairs with the largest dopant in the clusters. Dopant-interstitial clusters preferentially emit dopant-interstitial pairs with the smallest dopant. When several *n*-type dopant species are present in the same area of a semiconductor device, their diffusion and activation will be modified because of their direct and indirect interactions.

By performing calculations for a subset of the defects with increased accuracy, we estimated the numerical errors and showed that the observed trends are independent of the computational details. An in-depth analysis of the implications of the clustering energetics by means of KMC simulations might indicate that further defects play a crucial role. The corresponding *ab initio* calculations must be performed with the same computational setup, in order to maintain the consistency in the database of *ab initio* results.

The energetics of a subset of our results (P-based clusters) have already been implemented in a KMC-based process simulator and tested with experimental data.[34] The clustering energetics did not require calibration (they were used unchanged) to perform well, even better than other parts of the complete KMC model. This demonstrates the usefulness and the validity of our approach.

ACKNOWLEDGMENTS

This work was supported by a grant from the Swiss National Supercomputing Centre CSCS. We wish to acknowledge useful discussions with Ch. Zechner and N. Zographos from Synopsys Switzerland LLC. This research was supported by the Swiss innovation promotion agency CTI.

[1] N. S. Bennett, N. E. B. Cowern, A. J. Smith, R. M. Gwilliam, B. J. Sealy, L. O'Reilly, P. J. McNally, G. Cooke, and H. Kheyrandish, Appl. Phys. Lett. **89**, 182122 (2006).
[2] N. S. Bennett, A. J. Smith, R. M. Gwilliam, R. P. Webb, B. J. Sealy, N. E. B. Cowern, L. O'Reilly, and P. J. McNally, J. Vac. Sci. Technol. B **26**, 391 (2008).
[3] H. C.-H. Wang, C.-C. Wang, C. H. Diaz, B.-K. Liew, J. Y.-C. Sun, and T. Wang, IEEE Trans. Electron Devices **49**, 67 (2002).
[4] C. C. Wang, T. Y. Huang, C. H. Diaz, C. H. Wang, R. Duffy, N. E. B. Cowern, and P. B. Griffin, *2003 IEEE International Conference on Simulation of Semiconductor Processes and Devices* (IEEE, New York, 2003).
[5] H.-D. Lee and Y.-J. Lee, IEEE Electron Device Lett. **20**, 42 (1999).
[6] W. Fichtner, J. Comput. Theor. Nanosci. **5**, 1089 (2008).
[7] C. S. Nichols, C. G. Van de Walle, and S. T. Pantelides, Phys. Rev. Lett. **62**, 1049 (1989).
[8] O. Sugino and A. Oshiyama, Phys. Rev. B **46**, 12335 (1992).
[9] O. Pankratov, H. Huang, T. Diaz de la Rubia, and C. Mailhiot, Phys. Rev. B **56**, 13172 (1997).
[10] J. S. Nelson, P. A. Schultz, and A. F. Wright, Appl. Phys. Lett. **73**, 247 (1998).
[11] X.-Y. Liu, W. Windl, K. M. Beardmore, and M. P. Masquelier, Appl. Phys. Lett. **82**, 1839 (2003).
[12] S. A. Harrison, T. F. Edgar, and G. S. Hwang, Appl. Phys. Lett. **87**, 231905 (2005).
[13] M. G. Ganchenkova, A. Y. Kuznetsov, and R. M. Nieminen, Phys. Rev. B **70**, 115204 (2004).
[14] S. A. Harrison, T. F. Edgar, and G. S. Hwang, Phys. Rev. B **74**, 195202 (2006).
[15] E. Rauls, Phys. Rev. B **74**, 075204 (2006).
[16] D. C. Mueller and W. Fichtner, Phys. Rev. B **70**, 245207 (2004).
[17] M. Ramamoorthy and S. T. Pantelides, Phys. Rev. Lett. **76**, 4753 (1996).
[18] J. Xie and S. P. Chen, J. Phys.: Condens. Matter **11**, 7219 (1999).
[19] J. Xie and S. P. Chen, J. Phys. D **32**, 1252 (1999).
[20] J. Xie and S. P. Chen, J. Appl. Phys. **87**, 4160 (2000).
[21] S. A. Harrison, T. F. Edgar, and G. S. Hwang, Phys. Rev. B **72**, 195414 (2005).
[22] S. A. Harrison, T. F. Edgar, and G. S. Hwang, Electrochem. Solid-State Lett. **9**, G354 (2006).
[23] Y. Kim, T. A. Kirichenko, N. Kong, L. Larson, and S. K. Banerjeea, Physica B **401-402**, 144 (2007).
[24] C. Ahn and S. T. Dunhan, Appl. Phys. Lett. **93**, 022112 (2008).
[25] D. C. Mueller, E. Alonso, and W. Fichtner, Phys. Rev. B **68**, 045208 (2003).
[26] Y. Kim, T. A. Kirichenko, N. Kong, G. Henkelman, and S. K. Banerjee, Phys. Rev. B **79**, 075201 (2009).
[27] L. Bai, D. Yu, G.-H. Lu, F. Liu, Q. Wang, and H. Yilmaz, Appl. Phys. Lett. **91**, 061926 (2007).
[28] B. Sahli and W. Fichtner, Phys. Rev. B **72**, 245210 (2005).
[29] C. G. Van de Walle, D. B. Laks, G. F. Neumark, and S. T. Pantelides, Phys. Rev. B **47**, 9425 (1993).
[30] G. Kresse and J. Hafner, Phys. Rev. B **47**, 558 (1993).
[31] G. Kresse and J. Furthmüller, Phys. Rev. B **54**, 11169 (1996).
[32] G. Kresse and D. Joubert, Phys. Rev. B **59**, 1758 (1999).
[33] H. J. Monkhorst and J. D. Pack, Phys. Rev. B **13**, 5188 (1976).
[34] B. Sahli, K. Vollenweider, N. Zographos, and C. Zechner, Mater. Sci. Eng., B **154-155**, 193 (2008).
[35] S. K. Estreicher, M. Gharaibeh, P. A. Fedders, and P. Ordejón, Phys. Rev. Lett. **86**, 1247 (2001).
[36] Y. A. Du, S. A. Barr, K. R. A. Hazzard, T. J. Lenosky, R. G. Hennig, and J. W. Wilkins, Phys. Rev. B **72**, 241306(R) (2005).
[37] Y. A. Du, R. G. Hennig, and J. W. Wilkins, Phys. Rev. B **73**, 245203 (2006).
[38] M. Posselt, F. Gao, and D. Zwicker, Nucl. Instrum. Methods Phys. Res. B **228**, 212 (2005).
[39] I. Martin-Bragado, M. Jaraiz, P. Castrillo, R. Pinacho, J. Barbolla, and M. M. De Souza, Phys. Rev. B **68**, 195204 (2003).